Probing Solvation-Shell Hydrogen Binding in Glassy and Sol−Gel Matrixes through Vibronic Sideband Luminescence Spectroscopy

Mahantesh S. Navati,[†] Anandhi Ray,[†] Jacob Shamir,[‡] and Joel M. Friedman*[,†]

Department of Physiology and Biophysics, Albert Einstein College of Medicine, Bronx, New York 10461, and Department of Chemistry, Hebrew University, Jerusalem, Israel

Received: September 4, 2003; In Final Form: November 10, 2003

The luminescence spectrum from Gd(III) contains vibronic sidebands that provide the vibrational frequencies of molecules that comprise the solvation shell surrounding this cation. The vibronic sidebands obtained from Gd(III) in porous sol−gel matrixes as a function of added glycerol and in trehalose-derived glassy matrixes are used to probe matrix- and solvent-induced changes in the hydrogen bonding between first- and second-shell solvent molecules. The results provide direct insight into the origin of the damped dynamics observed for guest proteins within these types of matrixes. The results are also consistent with the retention of water within the first solvation shell for both the glassy matrixes and the glycerol-bathed sol−gel.

Introduction

It is becoming evermore apparent that surface hydration effects play an essential role in modulation of protein structure, dynamics, and function. Despite the considerable interest in the influence of hydration-shell waters on protein behavior, detailed molecular level insights derived from experimental protocols have been slow to emerge. Recent time-resolved measurements have provided the promise of being able to monitor altered dynamics associated with site-specific hydration waters.[1−3] Despite these advances and the impressive advances in theory,[4−8] there is a need for spectroscopic probes that can both expose those properties of the surface waters that give rise to the perturbed dynamics and test models of hydration derived from simulations and thermodynamics. The stability of a given water molecule on the surface of a protein is determined both by the interaction with the adjacent surface residues and the hydrogen-bond strength with the second-shell hydration-shell waters. Gd(III)-based vibronic sideband luminescence spectroscopy (VSBLS) can be used to probe both the identity of the molecules occupying the first solvent shell of this cation and the hydrogen bonding between solvent molecules in the first and second hydration shell. The application of this technique to proteins is made feasible because Gd(III), like other rare-earth cations, strongly binds to calcium binding sites on the surface of proteins.[9−13] Under these conditions, variation in the hydrogen-bonding properties of the bound waters can be attributed to changes between first- and second-shell solvent molecules. In this work, Gd(III)-based VSBLS is used to probe the influence of nonaqueous environments upon the hydration shell of solvated Gd(III) as a prelude to protein studies.

The behavior of biological molecules in confined environments is of interest from both biophysical and biotechnology perspectives. The encapsulation of biomolecules in porous sol−gels has been shown to hold considerable promise for the development of protein-based biosensors as well as for being a valuable tool to trap and characterize nonequilibrium protein structures.[14−22] Similarly, embedding proteins in glassy matrixes derived from sugars such as trehalose is of interest both as a method for preserving biomolecular pharmaceuticals and as a biophysical tool for modulating protein dynamics.[23−33] The as yet unresolved nature of the solvent environment within both the sugar−glass matrix and the porous sol−gel is believed to be a significant factor contributing to the emergent properties of these materials. In this work, VSBLS is used to characterize how these two classes of matrixes perturb the hydration shell of Gd(III) cations.

Vibronic Sideband Luminescence Spectroscopy. The vibrational spectrum of water molecules occupying the first solvation shell surrounding a cation can be used to probe solvation. This follows because the vibrational frequencies of the first-shell water molecules will reflect changes in their hydrogen bonding to outer-sphere solvent molecules. Raman and IR spectroscopy can in principle provide the detailed molecular information necessary to characterize the hydration shell surrounding a cation. Both techniques provide the vibrational frequencies of individual molecular moieties. Such information is valuable both as a molecular fingerprint and as a measure of bonding properties. However, it is difficult to find vibrational markers specific to solvent molecules occupying a solvation shell of an ion or a protein. Gd(III) VSBLS, as outlined below, provides a vibrational spectrum derived exclusively from molecules surrounding the rare-earth ion. As such, VSBLS is a potentially potent molecular-level probe of the solvation layer of Gd(III).

VSBLS is derived from the observation that for certain rare-earth ions (referred to as using the nonspecific designation of Ln(III)), there are weak vibronic (vibration plus electronic) sidebands associated with electronic transitions detected in either the luminescence or the excitation spectrum.[34−36] These vibronic sidebands (VSB) correspond to transitions where there is a change in both the electronic state of the Ln(III) ion and the vibrational state of nearby molecules (analogous to lattice phonons in the case of solid state materials). Subtracting the energy of the electronic transition from that of the composite vibronic transition yields the energy or frequency of the

* Author to whom correspondence may be addressed. Telephone: (718) 430-3591. Fax: (718) 430-8819. E-mail: jfriedma@aecom.yu.edu.
[†] Albert Einstein College of Medicine.
[‡] Hebew University.

10.1021/jp0366466 CCC: $27.50
Published on Web 12/31/2003

vibrational transition. This vibrational frequency is the same frequency that would be obtained from an IR absorption spectrum if the appropriate binding site-specific absorption bands could be unambiguously identified or targeted. Such IR or Raman targeting cannot be done in any routine fashion.

Pertinent facts associated with VSBLS derived from earlier studies [35] include: (i) The relevant interactions are very short range, falling off as $1/R$.[6] As a consequence, the VSBs are reflective of only the nearest neighbors of the Ln(III) ion. (ii) The intensity of the VSB is proportional to the infrared oscillator strength of the vibrational transition and not to either the strength of the electronic transition or any Franck−Condon factor. (iii) The vibronic energy is, to a first approximation, the sum or difference of participating transitions. (iv) The participating vibrations are characteristic of the bond-stretching motions of coordinating or nearby molecules and do not necessarily involve those modes reflecting motion of the Ln(III) ion.

Gd(III) displays a luminescence spectrum that arises overwhelmingly from a single transition, $^6P_{7/2} \rightarrow {}^6S_{7/2}$ at ∼308 nm. The vibronic sideband spectrum associated with this electronic transition is not complicated by spectral congestion of the kind seen for Tb(III)[35] or Eu(III).[10] The luminescence from Gd(III) requires excitations in the near ultraviolet. The lowest-energy absorption band at ∼308 nm, which is also the location of the electronic origin of the luminescence spectrum, is spectrally sharp but very weak. There are several more intense absorption bands on the high-energy side of the 308-nm band that can be used for excitation. The peak at ∼275 nm is the most intense of these bands but is still a typically weak f−f transition.

Haas and Stein [37]first demonstrated the appearance of the O−H stretching band in the vibronic sideband of the luminescence from aqueous Gd(III). In subsequent studies using Tb(III) [35] and Gd(III),[38] the O−H vibronic spectrum was used to expose the nature of the hydrogen bonding between the first and second hydration shells surrounding the Ln(III) ion. The latter study[33] also showed that the OH stretching in bulk water (using IR or Raman) is different from that of the water in the hydration shell of Gd(III), indicative of stronger hydrogen bonding between the first- and second-shell waters surrounding Gd(III) compared to the hydrogen bonding among waters in the bulk solution.

Subsequently there were reports of VSBs associated with ligands, including water molecules, of Gd(III) interacting with EDTA, rabbit muscle parvalbumin, phospholipids, and DNA [39] as well as alcohols, crown ethers, carbonate, phosphate, and several other assorted organic molecules.[40] There have also been studies using Yb(III)-derived VSBLSs to probe cation binding sites in select proteins.[41]

In the present study, the frequency of the VSB arising from the OH stretching mode (at ∼3400 cm^{-1}) is used as a measure of matrix- and solvent-induced changes in the hydrogen bonding between first-shell waters and the second-sphere solvent molecules. A decrease or increase of this frequency is correlated with an increase or decrease in hydrogen-bond strength, respectively, between the first-shell waters and the second-shell molecules. The width of this band is used as a rough indication of the degree of heterogeneity associated with the distribution profile of hydrogen-bond strengths for the first-shell waters.

Experimental Methods

Trehalose and gadolinium chloride were purchased from Aldrich chemicals and used without further purification. The solution phase studies were conducted using a 0.1 M aqueous solution of gadolinium chloride ($GdCl_3$) in either H_2O or D_2O.

Preparation of Glassy Films. Trehalose (100 mg) was dissolved in 1.0 mL of a 1.0 M gadolinium chloride solution. A volume of this solution was added to a 1-cm path length optical quartz cuvette sufficient to form a thin layer on one face of the horizontally positioned cuvette. The horizontally positioned cuvette was dried under a mild vacuum in a desiccator until it formed a hard transparent film on the bottom wall of the cuvette. This drying process required several hours (10−20). Variations of this protocol included (i) using 50 mg of trehalose and 50 mg of either sucrose or dextran (70 000 Da) instead of the 100 mg trehalose and (ii) replacing the 1.0 M Gd solution with a solution that is 0.2 M in $MgCl_2$ as well as 1.0 M $GdCl_3$. The inclusion of dextran or sucrose in the glass is known to increase or decrease the glass transition temperature, respectively. The introduction of $MgCl_2$ was motivated by the observation that among several mono- and divalent cation chlorides, the magnesium salt had the largest influence on the properties of trehalose-derived glasses.[42−44]

A second protocol was also used in generating glassy matrixes. For this protocol, a small volume of the solution was added to a 10 mm diameter quartz NMR tube (Wilmad) and spun at sufficient velocity to maintain a thin layer of solution on the bottom 2−3 cm of the tube. The sample was rapidly dried under a steady stream of dry nitrogen (30 min). For this protocol, it was found that superior optical quality glasses could be generated using 200 mg (instead of 100 mg in the first protocol) of sugar/polysaccharide per 1.0 mL of 1.0 M $GdCl_3$ stock solution.

Preparation of Sol−Gel-Encapsulated Gd(III). Preparation of sol−gel-encapsulated Gd(III) samples consisted of two steps, an initial hydrolysis of the sol−gel precurser and a gelation process leading to sol−gel blocks or films. Tetramethyl orthosilicate (TMOS) is hydrolyzed by sonicating a mixture of 1.0 mL TMOS (Aldrich), 0.050 mL deionized water, and 0.040 mL of 2 mM HCl in an ice bath for 30 min to yield a clear solution. An aliquot of 500 μL of hydrolyzed TMOS is mixed with 2.0 mL of a 1 M $GdCl_3$ stock solution in either H_2O or D_2O. The mixture is then poured into a 1-cm quartz cuvette, sealed, and set aside during the gelation phase. Sol−gel blocks were prepared by adding sufficient material to fill approximately one third of the cuvette. Films of various thickness were prepared by adding sufficient material to cover one window of a horizontally positioned cuvette. The time of gelation at room temperature (RT) was from 30 min to several hours, depending on the thickness of the gel. The resulting sol−gels were optically clear and without any visible excess of solvent.

The results described below were obtained from two different samples. One sample consisted of a sol−gel monolith occupying the bottom third of a standard 10-mm cuvette. This sample was prepared using $GdCl_3$ in D_2O in the initial gelation phase. The sample was aged for 1 day and then covered with an excess of glycerol (100%). After 7 days, the glycerol was replaced with H_2O (using repetitive flushing). After several days, the water was again replaced with an excess of glycerol (100%). The second sample was prepared as a thick film (∼0.3 cm) sol−gel sample derived from $GdCl_2$ in H_2O. After the sample aged for 2 days, it was bathed in a 75% glycerol/water (by volume) mixture. After a temperature cycle (RT → ice bath → RT), the 75% glycerol solvent was replaced with 100% glycerol. The sample was then subjected to a series of temperature cyclings that included RT → ice bath → RT and RT → liquid N_2 → RT. Luminescence spectra were recorded during select moments during these temperature cycling and solvent replacement protocols.

Fluorescence Measurements. Luminescence spectra were recorded on both a QuantaMaster Model QM-2000-4SE enhanced performance scanning spectrofluorometer (Photon Technology International, Lawrenceville, NJ) and an RF-5301PC spectrofluorometer (Shimadzu Scientific Instruments, Princeton, NJ). The luminescence was excited with light in the region between 270 and 280 nm and the emission recorded from 290 to 400 nm. Excitation profiles for observed spectral peaks were routinely conducted to identify which peaks are unambiguously derived from Gd(III), solvent Raman scattering, and non-Gd-derived fluorescence. The sample chamber was configured for either front face or 90° excitations depending on the sample. The former configuration was used for thin glassy films, whereas the latter configuration was used with solution phase samples and thick but optically clear blocks of sol−gel. The luminescence spectra were recorded using a constant scan step size of 0.5 nm. The emission monochromator slits were set at 0.25 and 1.5 mm for scanning the relatively intense and sharp 308 nm and the much less intense and broader vibronic sidebands (between 320 and 350 nm), respectively. The observed Gd(III) luminescence resembles the previously reported spectra. The luminescence spectra consists of a relatively intense band at 308 nm assigned to the electronic transition and weaker bands between 320 and 360 nm attributed to the VSBs. The luminescence spectra are plotted as intensity (arbitrary units) vs frequency shift (cm^{-1}) from the electronic band at 308 nm (set as the zero point as is done for the laser excitation in Raman scattering.

The temperature dependence of the spectrum for trehalose−glass-embedded Gd(III) was studied using heating tape (Omegalux) and a control unit to progressively heat glassy samples (on the window of a cuvette) situated within the fluorometer from 30 to 80 °C. Sol−gel samples bathed in a large excess of glycerol were cooled in water−ice or liquid nitrogen baths from a few minutes to hours. The cooled samples were rapidly transferred to a dry nitrogen purged fluorometer, and the spectrum was immediately recorded.

A peak fit program (VER.4 from SPSS.INC) was used for background subtraction, smoothing the data and peak analyses.

Results

Gd(III) in H_2O and D_2O. Figure 1 shows segments of the 273-nm excited luminescence spectra of solution phase Gd(III) dissolved in H_2O and D_2O. The frequency values shown on the *x* axis in this and subsequent figures are the frequency shifts of the vibronic bands with respect to the electronic origin at ∼308 nm (same for H_2O and D_2O). The very much weaker VSB originating from the OH stretch of H_2O is shown at 344 nm, corresponding to a frequency shift of ∼3430 cm^{-1}. The OD stretch from D_2O can be seen at 333 nm, corresponding to a frequency shift of ∼2460 cm^{-1}. If a simple harmonic oscillator model is assumed, the ratio of these frequencies is exactly what one would expect from the isotope effect after accounting for the reduced mass of OH and OD. The error in the peak positions is estimated to be on the order of ±15 cm^{-1}. The intensity of the luminescence spectrum falls off dramatically as the excitation wavelength is shifted from 273 nm.

These spectra are similar to those reported earlier but with the origin at 308 nm instead of the reported 311 nm.[40] It was observed that if the scan speed for the fluorometer is too high, the sharp and intense origin band can get skewed toward 311 nm. The 308-nm value was obtained on two different fluorometers, and in both cases a slow scan speed proved critical in obtaining the accurate peak position. An accurate peak position is essential for evaluating the frequency shift of the vibronic sideband since the sideband, being much less intense and more broad (full width at half maximum (fwhm)), is very much less sensitive to the scan speed errors.

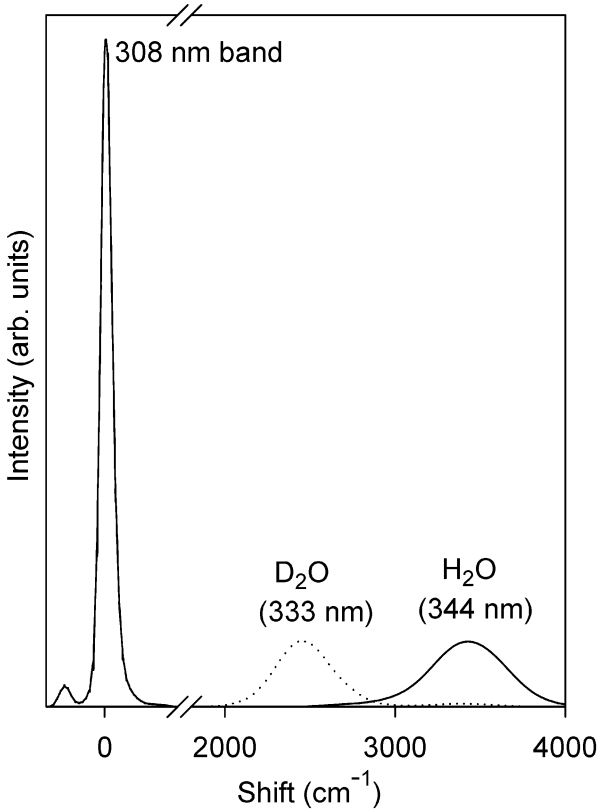

Figure 1. The 273-nm excited luminescence spectra from Gd(III) solutions in H_2O and D_2O. The emission slit width used to obtain the 308-nm band was 0.2 the width used to obtain both the OH and OD vibronic sidebands. The 308-nm bands derived from the two solutions were identical as measured.

Gd(III) in Sol−Gel Matrixes: The Effect of Gelation and of Added Glycerol. Figure 2 contains panels showing changes in the 273-nm excited VSBs from Gd(III) contained in a sol−gel monolith. Panels a and b are reference spectra from solution phase Gd(III) in D_2O and H_2O, respectively. The D_2O spectrum contains not only the VSB from the OD stretch but also a weak OH contribution from the few percent H_2O contaminant contained within the solution. The monolith was prepared using $GdCl_3$ in D_2O (as described in more detail in the methods section) to provide VSBs from both the OD and OH stretching modes. Panel c shows the OD and OH VSBs obtained immediately after gelation and before the addition of any bathing solvent. It can be seen that both the OD and OH stretching frequencies have shifted to higher values relative to the solution. The weak feature seen near 4000 cm^{-1} appears to be an overtone Raman band from the sol−gel based on its position and excitation wavelength dependence.

Panels d−f show the changes in the VSB as a function of time after the addition of a large excess (based on volume) of pure glycerol to the cuvette containing the monolith. Previous studies have shown that the addition of glycerol as a bathing medium to sol−gel-encapsulated proteins slows conformational dynamics.[18,31] Panels d−f show two progressive changes after glycerol addition. The first is an increase in the relative contribution of the OH sideband relative to the OD sideband. This change is reflective of the H−D exchange in the presence of the large excess of exchangeable protons from the added

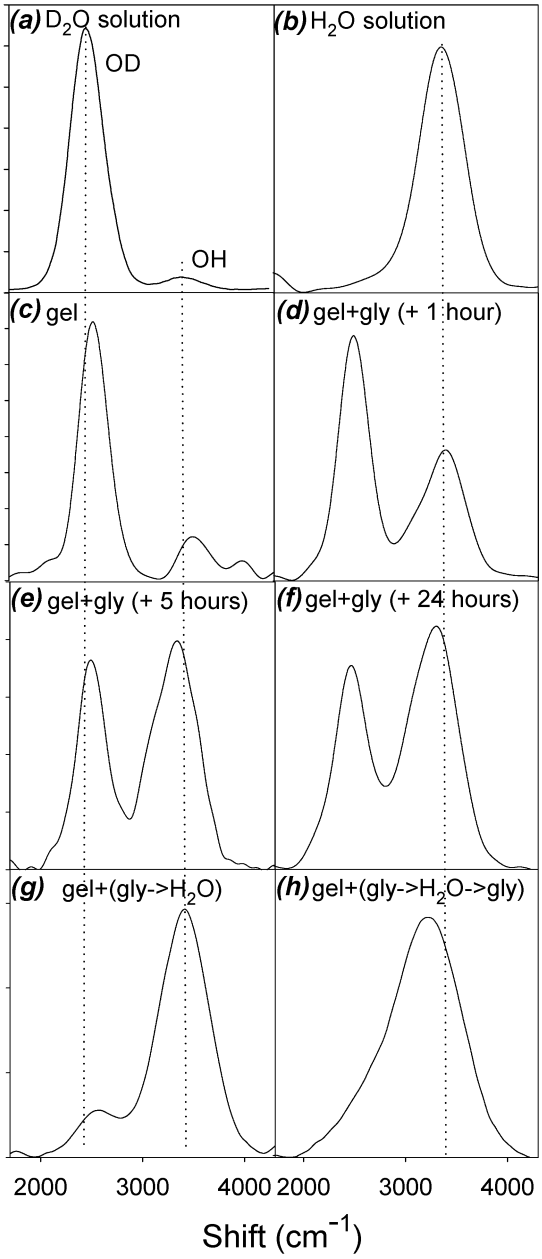

Figure 2. The evolution of the vibronic sidebands (VSB), ν(OH) and ν(OD), from Gd(III) (in) in a sol−gel monolith prepared using D_2O to which an excess of glycerol was added after gelation and aging. Panels a and b show the high-frequency VSBs from Gd(III) in D_2O and H_2O, respectively. Panels c, d, e, and f depict the OH and OD VSBs from Gd(III) in the monolith before adding glycerol, 1 h after adding glycerol, 5 h after adding glycerol, and 24 h after adding glycerol, respectively. In g, the spectrum was recorded after the glycerol-soaked sol−gel block was first extensively flushed with water and then bathed in an excess of water. In h, the spectrum was recorded after the water bathing the sol−gel block (as described for panel g) was replaced with an excess of glycerol.

glycerol. The other change is the progressive downshift with time of the frequency of both the OD and OH stretching modes. A summary of the frequency shifts is given in Table 1. As can be seen from the comparison of the day one and day seven spectra in Table 1, the peak positions remain stable after the first 24 h (however, the relative intensity of the OH band continues to increase). It should be noted that the positions and widths are derived from curve-fitting programs; however, the uncertainty in the actual numbers is estimated to be as large as several cm^{-1} due to the broadness of the bands involved.

TABLE 1: OH and OD Stretching Frequencies and Line Shape Widths (fwhm) Derived from the Vibronic Sidebands in the 273-nm Excited Luminescence Spectrum of Gd(III) in Solution and in a Sol−Gel Monolith to Which Glycerol Is Added

	$\Delta\nu$; Γ (in cm^{-1})	
conditions	D_2O band	H_2O band
solution (H_2O)		3429.2; 512.3
solution (D_2O)	2463.5; 369.8	3431.1; 273.7
sol−gel (D_2O)	2528.2; 337.6	3516.7; 280.9
$t = 0$ (+glycerol)	2494.6; 340.8	3447.6; 379.4
$t = 1$ h (+glycerol)	2489.7; 353.2	3362.7; 522.5
$t = 4$ h (+glycerol)	2480.2; 317.3	3323.3; 485.7
$t = 5$ h (+glycerol)	2503.5; 351.2	3321.4; 537.5
$t = 1$ day (+glycerol)	2473.4; 412.9	3274.5; 577.9
$t = 7$ days (+glycerol)	2472.9; 350.9	3284.0; 533.2
glycerol → H_2O		3442; 575.3
glycerol → H_2O → glycerol		3262.0; 675.2

Panel g in Figure 2 shows the effect when after 7 days the glycerol in the sol−gel monolith is flushed out and replaced with a large excess of H_2O. It can be seen from the figure as well as in Table 1 that the OH frequency is now, within experimental error, the same as for aqueous Gd(III). Replacing the added water with an excess of glycerol (panel h) results in the OH stretching frequency, resuming the previously obtained low value observed after the initial seven-day exposure to glycerol (see Table 1).

The viscosity of glycerol increases with decreasing temperature, as does the impact of added glycerol on the dynamics of sol−gel-encapsulated proteins. Figure 3 shows the OH stretching frequency in the vibronic spectrum of Gd(III) encapsulated in a thick film sol−gel sample as a function of temperature and time after the addition of an excess of glycerol. The initial sol−gel spectrum prior to the addition of glycerol (spectrum a) yields a peak frequency very similar to that of Gd(III) in solution. This result is in contrast to that obtained from the thick monolith at early time (with respect to gelation) where the frequency was higher than that for the solution. As observed for the previous sample, the vibronic OH stretching frequency decreases with the addition of glycerol. Spectrum b was obtained a few hours after the addition of the glycerol. Immersing this glycerol-containing several-hour-old sample in liquid N_2 for several minutes and then immediately generating the spectrum in a dry N_2 purged chamber within the fluorometer yields a larger downshift as seen for spectrum c. Allowing the glycerol sample to age for 3 days results in a spectrum d, which is comparably shifted as the liquid N_2 cycled sample (spectrum c). Repetition of the cooling cycle for the three-day-old sample produced no further shift in frequency. These frequency changes are summarized in Table 2. Similar treatment of a sample with an excess of 75% glycerol/water solution (by volume) resulted in similar behavior but with a smaller shift. It is to be noted that the intensity of the water band in all of the spectra did not show any substantial intensity decrease that would suggest a loss of water from the hydration shell of the Gd(III).

In contrast to the behavior observed in the glycerol-soaked sol−gel, the spectra from solutions of Gd(III) in 90 and 99% glycerol showed no change in the frequency of the OH stretching band. The weak VSB band at ~223 nm seen in the aqueous solution and assigned to the water bending mode remains fully discernible for both classes of glycerol-containing samples.

Gd(III) in Glassy Matrixes. Figure 4 shows the change in the OH-stretch VSB of Gd(III) in going from aqueous solution (spectrum a) to glassy matrixes derived from the slow drying of a trehalose solution (spectrum b) and of a trehalose and

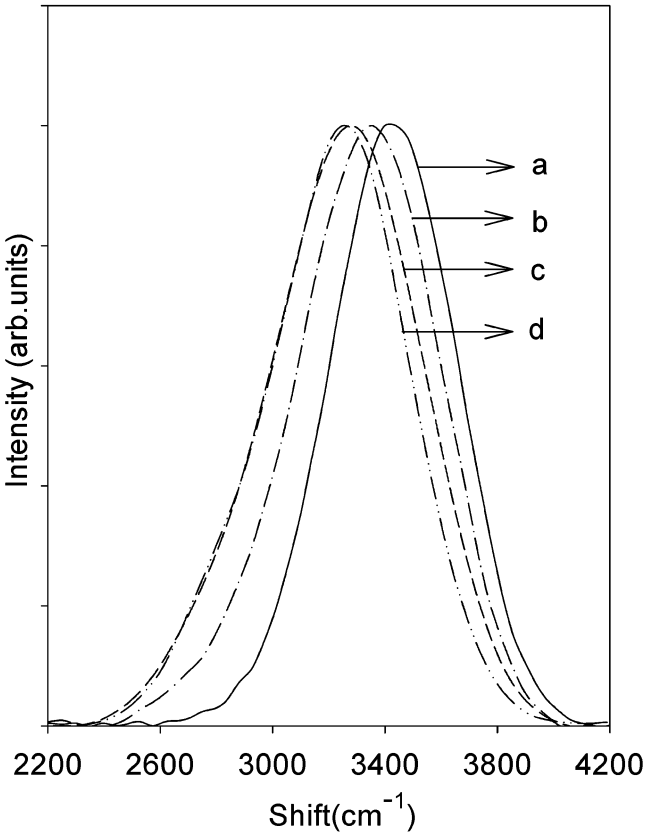

Figure 3. The OH VSB from Gd(III) in a thick sol−gel film immersed in an excess of glycerol. Spectrum a is from the film before adding glycerol. Spectra b and c are after soaking the sol−gel block in an excess of glycerol at RTfor 3 h and 3 days, respectively. In d, the VSB is generated from the sample after being immersed in glycerol for 3 h, cooled to 77 K for several minutes, and then probed while still cold (see test for details).

TABLE 2: OH Stretching Frequency Derived from the Vibronic Sideband Luminescence Spectrum of Gd(III) in Solution and in a Sol−Gel Film to Which Glycerol Is Added

conditions	OH band $\Delta\nu$ (cm^{-1})
solution (H_2O)	3429
sol−gel (thick film)	3429
sol−gel + 100% glycerol (~3 h, RT)	3340
sol−gel + 100% glycerol (3 days later, RT)	3263
sol−gel + 100% glycerol (~3 h, cooled)	3243

dextran solution (spectrum c). Relative to the solution spectrum, the OH stretching frequencies of the vibronic spectra from the glassy matrixes are shifted to higher frequency and the fwhm is markedly reduced. Similar results (not shown) were obtained from a slow-dried glassy matrix derived from a 50/50 mixture of trehalose and sucrose. For all these samples, the spectra show no noticeable decrease in the weak vibronic band assigned to the bending mode of water.

Samples prepared either by drying at ambient temperatures or by first drying and then heating in an oven at 60−70 °C for 40 min to an hour show very little difference in the frequency and width of the VSB measured at ambient temperatures. Ramping the temperature between 30 and 80 °C for an air-exposed trehalose-derived glassy sample while collecting sequential spectra revealed that with heating there is a progressive but modest decrease in the intensity of the VSB relative to the electronic band, indicative of a loss of hydration water with heating. When normalized with respect to intensity, the VSBs detected at different temperatures show minimal change in

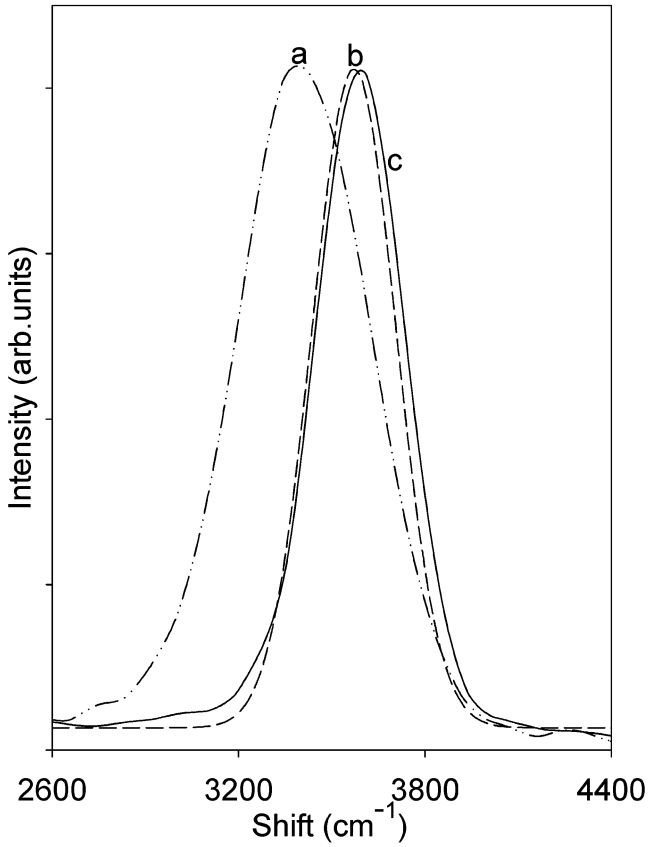

Figure 4. The OH VSB from Gd(III) in aqueous solution (a), trehalose glass (b), and trehalose plus dextran glass (c).

frequency or line shape, indicating that in the glassy matrix, even as water is lost, the remaining first-shell hydration waters maintain the same degree of interaction with the second-shell solvent molecules. As the temperature is allowed to return back toward ambient levels, the VSB intensity reverted back to the original value.

Not shown are the results from the rapidly dried samples. In contrast to the slowly dried samples, these samples showed very little change in both line shape and frequency compared to the solution phase sample.

Figure 5 shows that the inclusion of $MgCl_2$ in the trehalose-derived glassy matrix perturbs the pattern observed for the $MgCl_2$-free glass. It can be seen from spectrum c that the vibronic spectrum is now further blueshifted and the width of the band is greatly increased. A much smaller frequency shift and a smaller degree of line broadening is seen for the corresponding $MgCl_2$ containing solution. The above results from the glassy matrixes are summarized in Table 3.

Discussion

The above results indicate that Gd(III) retains a large fraction of its hydration-shell waters when exposed to several extreme solvent perturbations. However, in each of these instances, the frequency behavior of the OH stretching frequency reveals distinct differences in the interactions between retained first-shell waters and second-shell solvent molecules.

The VSB OH stretching frequency in aged sol−gel matrixes is minimally perturbed compared to aqueous solution. This result is consistent with Gd(III) occupying the water-filled pores that permeate hydrogels. The observation of an initial blueshifted OH frequency for Gd(III) in a newly prepared sol−gel monolith, indicating that during the early stages of gelation (but not after

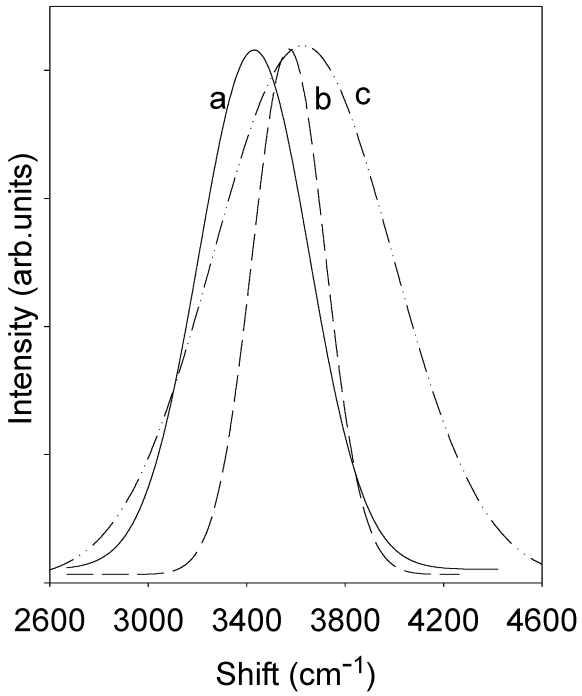

Figure 5. The OH VSB from Gd(III) in aqueous solution (a), trehalose glass (b), and trehalose plus $MgCl_2$ glass (c).

TABLE 3: OH Stretching Frequency and Line Shape Width (fwhm) Obtained from the Vibronic Sidband Luminescence Spectrum of Gd(III) in Glassy Matrices

sample environment	$\Delta\upsilon$; Γ (cm^{-1})
solution	3429; 512
glass (trehalose)	3572; 270
glass (trehalose + Mg(II))	3629; 731
solution + Mg(II)	3458; 537
glass (trehalose + dextran)	3591; 284
glass (trehalose + sucrose)	3572; 297

aging), hydrated Gd(III) is exposed to an environment that is distinctly different from bulk water possibly due to the production of methanol during gelation.

The effect of added glycerol on the hydration shell of sol−gel-encapsulated Gd(III) is different from that of Gd(III) in solution. In solution, the addition of an extreme excess of glycerol produces no discernible shift in the VSB OH stretching frequency. In contrast, the addition of glycerol to the sol−gel-encapsulated Gd(III) even at lower concentration levels engenders a decrease in the OH stretching frequency. The magnitude of the decrease appears to increase both with the fractional content of glycerol added to the sol−gel and, at intermediate values, with decreasing temperature. The results imply a limiting value achievable with either high concentrations of glycerol or reduced temperature when the concentration of glycerol is not sufficient to produce the maximum effect at ambient temperatures. Thus the environment within the sol−gel matrix facilitates what appears to be a greatly enhanced glycerol effect that is manifested as increased hydrogen binding between surface waters and the second shell solvent molecules. It is plausible that relative to the free solution, the confined volume and dielectric properties associated with the pores in the sol−gel favor a modified configuration or composition of the second shell when glycerol is added.

It has been shown that the addition of glycerol to sol−gel-encapsulated proteins damps conformational dynamics far beyond what occurs in free solutions containing similar concentrations of glycerol.[18,31] The present results show that in the sol−gel, glycerol enhances the hydrogen binding between first- and second-shell solvent molecules. Many studies have implicated the dynamics of surface waters as being critical for certain categories of protein motion.[5−7,24,25,33,45−50] The present results support the idea that the glycerol effect in the sol−gel originates from an enhanced stability of the first-shell waters thereby limiting the dynamics of the surface waters that in turn slow the protein dynamics that are slaved to those of the hydration shell.

Glycerol added to sol−gel-encapsulated proteins causes similar damping of conformational dynamics as is seen for protein in glassy matrixes.[7,26,28,29,33,51,52] Despite the similar effect on dynamics, the present results show that the nature of the hydration shell under these two conditions is different. Whereas the hydrogen bonding between first- and second-shell molecules is enhanced with added glycerol, the formation of a glass derived from trehalose is associated with a general weakening of these bonds but with a dramatic narrowing of the distribution of hydrogen bond strengths. The trehalose result indicates that the surface waters are retained in the glass as predicted by simulations for proteins[25] and that these hydration waters are clearly incorporated into the extended and well-defined hydrogen-bonding network associated with the glass. Under these glassy conditions, diminished hydration shell dynamics are likely to arise because of enthalpically unfavorable transition-state species in which the hydrogen bonding network must be transiently disrupted in order for a water molecules to shift sites on the surface of the protein.

The glass-induced decrease in the hydrogen-bond strength between the first- and second-shell waters is likely due to one of two possibilities. One possibility is that the ordering of trehalose and water within the glassy matrix limits the ability of second-shell solvent molecules to adopt an optimum geometry with respect to maximizing hydrogen bonding to the waters in the first hydration shell. A second possibility is that the molecules capable of hydrogen bonding to the first-shell hydration waters are strongly hydrogen bonded to the molecules participating in the formation of the glassy matrix and are therefore not capable of forming a strong hydrogen bond with the hydration-shell waters of the Gd(III).

On the basis of the similar frequencies and line widths observed (see Table 3) in the VSB spectra in the glassy matrixes derived from trehalose, trehalose plus sucrose, and trehalose plus dextran, the properties of the hydration shell are not noticeably sensitive to factors that alter the glass transition temperature. It is clear that the addition of $MgCl_2$ causes a major alteration in the hydrogen-bonding network of the glass as reflected both in the large increase in line shape and in the increase in the VSB OH stretching frequency compared to the $MgCl_2$-free glassy matrixes. This effect is likely the consequence of the high charge density associated with Mg(II) that results in its hydration waters being very tightly bound.[53] This strong interaction should decouple its hydration waters from the surrounding environment thereby decreasing the local viscosity as is observed.[44] In addition, this decoupling of the Mg(II) hydration waters should also result in a decrease in the concentration of water molecules available to participate in extended hydrogen-bonding networks thus creating local inhomogeneities within the glass and perhaps an overall decrease in the rigidity of the glassy matrix.

Conclusions

The presented results show that Gd(III)-based vibronic sideband luminescence spectroscopy can be used to probe

solvent-induced perturbations of the hydration waters of Gd(III). The spectra of Gd(III) in glycerol-loaded sol−gel matrixes and trehalose-derived glassy matrixes are consistent with preferential hydration models in which glycerol and sugars are excluded from the first-shell hydration layer.[8] The results have implications for how protein motions are damped in different high viscosity matrixes. Damping of solvent-slaved protein dynamics for sol−gel-encapsulated samples to which glycerol is added is likely due to stabilization of first-shell waters due to enhanced hydrogen binding to second-shell solvent molecules. In contrast, it appears that within trehalose-derived glassy matrixes, it is the destabilization of transition-state conformations in which the surface water becomes transiently decoupled from the hydrogen-bonding network of the glass.

Since Gd(III) effectively binds to calcium binding sites in proteins, the approach used in the present study should be applicable to studies of solvent-induced perturbations of the hydration layer of proteins in the immediate vicinity of cation-occupied calcium binding sites. In addition, appropriate chelating agents tethered to specific sites on the surface of proteins can be used to probe the hydration layer at varying distances from the protein surface.

Acknowledgment. This work was supported through funding from the National Institutes of Health (R01 EB00296) and the W.M. Keck Foundation.

References and Notes

(1) Pal, S. K.; Peon, J.; Zewail, A. H. *Proc. Natl. Acad. Sci. U. S. A.* **2002**, *99*, 1763.
(2) Pal, S. K.; Peon, J.; Zewail, A. H. *Proc. Natl. Acad. Sci. U. S. A.* **2002**, *99*, 15297.
(3) Changenet-Barret, P.; Choma, C. T.; Gooding, E. F.; DeGrado, W. F.; Hochstrasser, R. M. *J. Phys. Chem. B* **2000**, *104*, 9322.
(4) Timasheff, S. N. *Biochemistry* **1992**, *31*, 9857.
(5) Tarek, M.; Tobias, D. J. *Phys. Rev. Lett.* **2002**, *89*, 275501.
(6) Tarek, M.; Tobias, D. J. *Phys. Rev. Lett*. **2002**, *88*, 138101.
(7) Vitkup, D.; Ringe, D.; Petsko, G. A.; Karplus, M. *Nat. Struct. Biol.* **2000**, *7*, 34.
(8) Timasheff, S. N. *Biochemistry* **2002**, *41*, 13473.
(9) Cronce, D. T.; Horrocks, W. D., Jr. *Biochemistry* **1992**, *31*, 7963.
(10) Horrocks, W. D., Jr. *Methods Enzymol*. **1993**, *226*, 495.
(11) Sudnick, D. R.; Horrocks, W. D., Jr. *Biochim. Biophys. Acta* **1979**, *578*, 135.
(12) Wang, C. L.; Leavis, P. C.; Horrocks, W. D., Jr.; Gergely, J. *Biochemistry* **1981**, *20*, 2439.
(13) Martin, R. B.; Richardson, F. S. *Q. Rev. Biophys.* **1979**, *12*, 181.
(14) Bettati, S.; Mozarrelli, A. *J. Biol. Chem.* **1997**, *272*, 32050.
(15) Das, T. K.; Khan, I.; Rousseau, D. L.; Friedman, J. M. *Biospectroscopy* **1999**, *5*, S64.
(16) Eggers, D. K.; Valentine, J. S. *Protein Sci.* **2001**, *10*, 250.
(17) Ellerby, L. M.; Nishida, C. R.; Nishida, F.; Yamanaka, S. A.; Dunn, B.; Valentine, J. S.; Zink, J. I. *Science* **1992**, *255*, 1113.
(18) Khan, I.; Shannon, C. F.; Dantsker, D.; Friedman, A. J.; Perez-Gonzalez-de-Apodaca, J.; Friedman, J. M. *Biochemistry* **2000**, *39*, 16099.
(19) Shibayama, N. A. S. S. *J. Mol. Biol.* **1995**, *251*, 203.
(20) Dave, B. C.; Dunn, B.; Valentine, J. S.; Zink, J. I. *Anal. Chem.* **1994**, *66*, 1120A.
(21) Gill, I.; Ballesteros, A. *Ann. N. Y. Acad. Sci.* **1996**, *799*, 697.
(22) Navati, M. S.; Samuni, U.; Aisen, P.; Friedman, J. M. *Proc. Natl. Acad. Sci. U. S. A.* **2003**, *100*, 3832.
(23) Cordone, L.; Galajda, P.; Vitrano, E.; Gassmann, A.; Ostermann, A.; Parak, F. *Eur. Biophys. J. Biophys. Lett.* **1998**, *27*, 173.
(24) Cordone, L.; Ferrand, M.; Vitrano, E.; Zaccai, G. *Biophys. J.* **1999**, *76*, 1043.
(25) Cottone, G.; Cordone, L.; Ciccotti, G. *Biophys. J.* **2001**, *80*, 931.
(26) Dantsker, D.; Samuni, U.; Friedman, A. J.; Yang, M.; Ray, A.; Friedman, J. M. *J. Mol. Biol*. **2002**, *315*, 239.
(27) Elbein, A. D.; Pan, Y. T.; Pastuszak, I.; Carroll, D. *Glycobiology* **2003**, *13*, 17.
(28) Gottfried, D.; Peterson, E.; Sheikh, A.; Yang, M.; Wang, J.; Friedman, J. *J. Phys. Chem.* **1996**, *100*, 12034.
(29) Hagen, S. J.; Hofrichter, J.; Eaton, W. A. *Science* **1995**, *269*, 959.
(30) Lillford, P. J.; Holt, C. B. *Philos. Trans. R. Soc. London, Ser. B* **2002**, *357*, 945.
(31) Samuni, U.; Dantsker, D.; Ray, A.; Wittenberg, J. B.; Wittenberg, B. A.; Dewilde, S.; Moens, L.; Ouellet, Y.; Guertin, M.; Friedman, J. M. *J. Biol. Chem*. **2003**.
(32) Wright, W. W.; Carlos Baez, J.; Vanderkooi, J. M. *Anal. Biochem.* **2002**, *307*, 167.
(33) Librizzi, F.; Viappiani, C.; Abbruzzetti, S.; Cordone, L. *J. Chem. Phys.* **2002**, *116*, 1193.
(34) Freed, S. *Rev. Mod. Phys.* **1942**, *14*, 105.
(35) Stavola, M.; Isganitsis, L.; Sceats, M. G. *J. Chem. Phys.* **1981**, *74*, 4228.
(36) Yatsiv, S.; Ehrenfreund, E.; El-Hanany, U. *J. Chem. Phys.* **1965**, *42*, 743.
(37) Haas, Y.; Stein, G. *Chem. Phys. Lett.* **1971**, *15*, 143.
(38) Stavola, M.; Friedman, A. J.; Stepnoski, R. A.; Sceats, M. G. *Chem. Phys. Lett.* **1981**, *80*, 192.
(39) Iben, I. E.; Stavola, M.; Macgregor, R. B.; Zhang, X. Y.; Friedman, J. M. *Biophys. J.* **1991**, *59*, 1040.
(40) MacGregor, R. B., Jr. *Arch. Biochem. Biophys.* **1989**, *274*, 312.
(41) Mattioli, T. A.; Roselli, C.; Boussac, A. *Biochim. Biophys. Acta* **1992**, *1101*, 121.
(42) Mazzobre, M. F.; Longinotti, M. P.; Corti, H. R.; Buera, M. P. *Cryobiology* **2001**, *43*, 199.
(43) Mazzobre, M. F.; Del Pilar Buera, M. *Biochim. Biophys. Acta* **1999**, *1473*, 337.
(44) Mazzobre, M. F.; Fucito, S.; Corti, H. R.; Buera, M. P. Sugar−saltwater interactions and their role on biomolecular stabilization; *J. Biotechnol*. www.ejbiotechnology.info/feedback/proceedings/04/poster/p23.html, ISSN-0717-3458, 2000.
(45) Frauenfelder, H.; Fenimore, P. W.; McMahon, B. H. *Biophys. Chem.* **2002**, *98*, 35.
(46) Lichtenegger, H.; Doster, W.; Kleinert, T.; Birk, A.; Sepiol, B.; Vogl, G. *Biophys. J.* **1999**, *76*, 414.
(47) Kleinert, T.; Doster, W.; Leyser, H.; Petry, W.; Schwarz, V.; Settles, M. *Biochemistry* **1998**, *37*, 717.
(48) Doster, W.; Cusack, S.; Petry, W. *Nature* **1989**, *337*, 754.
(49) Reat, V.; Dunn, R.; Ferrand, M.; Finney, J. L.; Daniel, R. M.; Smith, J. C. *Proc. Natl. Acad. Sci. U. S. A.* **2000**, *97*, 9961.
(50) Teeter, M. M.; Yamano, A.; Stec, B.; Mohanty, U. *Proc. Natl. Acad. Sci. U. S. A.* **2001**, *98*, 11242.
(51) Hagen, S. J.; Hofrichter, J.; Eaton, W. A. *J. Phys. Chem.* **1996**, *100*, 12008.
(52) Rector, K. D.; Jiang, J. W.; Berg, M. A.; Fayer, M. D. *J. Phys. Chem. B* **2001**, *105*, 1081.
(53) Collins, K. D. *Biophys. J.* **1997**, *72*, 65.